Check for updates

LIMNOLOGY and OCEANOGRAPHY

ASLO

Limnol. Oceanogr. 67, 2022, 135–146
© 2021 The Authors. *Limnology and Oceanography* published by Wiley Periodicals LLC on behalf of Association for the Sciences of Limnology and Oceanography.
doi: 10.1002/lno.11981

Oxygen-deficient water zones in the Baltic Sea promote uncharacterized Hg methylating microorganisms in underlying sediments

Eric Capo,[1,2*] **Elias Broman**,[3,4] **Stefano Bonaglia**,[3,5] **Andrea G. Bravo**,[6] **Stefan Bertilsson**,[2] **Anne L. Soerensen**,[7] **Jarone Pinhassi**,[8] **Daniel Lundin**,[8] **Moritz Buck**,[2] **Per O. J. Hall**,[5] **Francisco J. A. Nascimento**,[3,4] **Erik Björn**[1]

[1]Department of Chemistry, Umeå University, Umeå, Sweden
[2]Department of Aquatic Sciences and Assessment, SLU Uppsala, Uppsala, Sweden
[3]Department of Ecology, Environment and Plant Sciences, Stockholm University, Stockholm, Sweden
[4]Baltic Sea Centre, Stockholm University, Stockholm, Sweden
[5]Department of Marine Sciences, University of Gothenburg, Gothenburg, Sweden
[6]Department of Marine Biology and Oceanography, Institute of Marine Sciences, Spanish National Research Council (CSIC), Barcelona, Spain
[7]Department of Environmental Research and Monitoring, Swedish Museum of Natural History, Stockholm, Sweden
[8]Centre for Ecology and Evolution in Microbial Model Systems - EEMiS, Linnaeus University, Kalmar, Sweden

Abstract

Human-induced expansion of oxygen-deficient zones can have dramatic impacts on marine systems and its resident biota. One example is the formation of the potent neurotoxic methylmercury (MeHg) that is mediated by microbial methylation of inorganic divalent Hg (Hg^{II}) under oxygen-deficient conditions. A negative consequence of the expansion of oxygen-deficient zones could be an increase in MeHg production due to shifts in microbial communities in favor of microorganisms methylating Hg. There is, however, limited knowledge about Hg-methylating microbes, i.e., those carrying *hgc* genes critical for mediating the process, from marine sediments. Here, we aim to study the presence of *hgc* genes and transcripts in metagenomes and metatranscriptomes from four surface sediments with contrasting concentrations of oxygen and sulfide in the Baltic Sea. We show that potential Hg methylators differed among sediments depending on redox conditions. Sediments with an oxygenated surface featured *hgc*-like genes and transcripts predominantly associated with uncultured Desulfobacterota (OalgD group) and Desulfobacterales (including *Desulfobacula* sp.) while sediments with a hypoxic-anoxic surface included *hgc*-carrying Verrucomicrobia, unclassified Desulfobacterales, Desulfatiglandales, and uncharacterized microbes. Our data suggest that the expansion of oxygen-deficient zones in marine systems may lead to a compositional change of Hg-methylating microbial groups in the sediments, where Hg methylators whose metabolism and biology have not yet been characterized will be promoted and expand.

Methylmercury (MeHg) is a highly neurotoxic compound that biomagnifies in aquatic food webs and can endanger human health following consumption of Hg-contaminated seafood (Mason et al. 2012). In the environment, the formation of MeHg is predominantly mediated by microbial methylation of inorganic divalent mercury (Hg^{II}) into MeHg at oxygen-deficient conditions (Bravo and Cosio 2019; Bowman et al. 2020; Tang et al. 2020). Certain sulfate-reducing bacteria, iron-reducing bacteria, methanogens, and fermenters have been identified as key mediators of this biological process (Compeau and Bartha 1985; Fleming et al. 2006; Hamelin et al. 2011; Bravo et al. 2018). Microbial Hg methylation was recently found to be associated with *hgc* genes—*hgcA* and *hgcB*—coding for, respectively, a corrinoid protein and a ferredoxin (Parks et al. 2013). Since this discovery, numerous studies have characterized the diversity of *hgc*-carrying microbes that are found in oxygen-deficient environments (e.g., rice

*Correspondence: eric.capo@hotmail.fr

This is an open access article under the terms of the Creative Commons Attribution-NonCommercial-NoDerivs License, which permits use and distribution in any medium, provided the original work is properly cited, the use is non-commercial and no modifications or adaptations are made.

Additional Supporting Information may be found in the online version of this article.

Author Contribution Statement: E.C. and E.B. contributed equally to this work. F.J.A.N. and E.B. are joint last authors of this work.

paddies, wetlands, lake sediments, and anoxic waters; Bravo and Cosio 2019) and this search has considerably advanced the understanding of the diversity of microbes with the potential to methylate Hg. Recent studies have, for example, highlighted the capacity of certain syntrophs to perform Hg methylation in oxygen-deficient environments (Yu et al. 2018; Hu et al. 2020; Peterson et al. 2020).

Marine sediments have long been recognized as an environmental compartment with active Hg methylation (Gilmour et al. 1998; King et al. 1999, 2000, 2001; Hollweg et al. 2009, 2010; Merritt and Amirbahman 2009; Azaroff et al. 2019). More specifically, the oxygen-deficient conditions of seafloor sediments (sometimes called "dead zones"), which feature high levels of dissolved sulfide, are expected to be suitable habitats for putative Hg methylators, such as *hgc*-carrying sulfate-reducing bacteria (Jones et al. 2019; Lin et al. 2021). Such oxygen-deficient zones are expanding as a consequence of anthropogenic eutrophication of multiple water bodies (Conley et al. 2012; Breitburg et al. 2018), including the Baltic Sea which has seen a dramatic expansion of hypoxic-anoxic bottoms over the past 30 yr (Hansson et al. 2020). Today, this brackish system holds one of the largest oxygen-deficient areas in the world (Diaz and Rosenberg 2008). This might have severe implications for the formation of MeHg. Previous studies have reported the distribution and bioavailability of Hg (Kwasigroch 2021) as well as relatively high concentrations of MeHg in superficial sediments from estuaries and major basins of the Baltic Sea, with values ranging from 61 to 940 $pg.g^{-1}$ (Beldowski et al. 2014) and up to 2362 $pg.g^{-1}$ in offshore munition dumpsites (Siedlewicz et al. 2020). Although, rates of Hg methylation and taxonomic composition of microbes potentially involved in Hg methylation (i.e., harboring *hgc* genes) have recently been described in Baltic Sea hypoxic and anoxic water layers (Soerensen et al. 2018; Capo et al. 2020), little is known about potential Hg methylation in Baltic Sea sediments, and in particular how different oxygen and sulfide concentrations affect Hg methylation and the microorganisms involved in the process.

One approach to gain insight about microbial Hg methylation capacity is to study the composition and the activity of Hg-methylating microbial groups. Shotgun metagenomics—based on sequencing of DNA found in a given environmental sample (e.g., water, soil, and sediment)—has emerged as a powerful tool to detect and identify *hgc* genes ad hoc (Gionfriddo et al. 2016; Bowman et al. 2020; Tada et al. 2020; Villar et al. 2020) notably because avoiding biases introduced by polymerase chain reaction amplification. Additionally, although there is some uncertainty regarding the relationships between the expression of *hgc* genes, Hg methylation rates, and MeHg concentrations (*see* Goñi-Urriza et al. 2015; Bravo et al. 2016; Christensen et al. 2019; Schaefer et al. 2020), the sequencing and quantification of *hgc* transcripts may provide complementary information about the dynamics and activity of Hg-methylating microbial groups and be important data to resolve their active participation in Hg methylation.

Considering that oxygen-deficient sediments are prone to Hg methylation (Bravo and Cosio 2019), it is plausible that an increase in oxygen-deficient areas provides an expanding niche for Hg methylators (Peñuelas et al. 2019). Here, we hypothesized that a decrease of oxygen in bottom waters, and hence in surface sediments, will lead to a shift in Hg-methylating microbial groups in the sediment. For instance, this would result in an increase of anaerobic microhabitats in the water column such as settling particles in which Hg methylators are suspected to thrive (Gascón Díez et al. 2016; Capo et al. 2020) that would fuel the sediment with Hg-methylating microbial groups from the water column. These particle-associated microorganisms would eventually reach the sediment and potentially induce a shift in the composition of resident Hg methylating microorganisms. By using metagenomic and metatranscriptomic sequencing from sediments exhibiting various levels of oxygen and sulfide concentrations, our study provides an expanded view on the diversity of *hgc*-carrying microbes and the geochemical conditions where these genes and organisms are active. Specifically, this study advances our understanding of potential compositional changes in Hg-methylating microbial groups following the expansion of oxygen-deficient marine zones.

Material and methods

Sediment sampling

Full details of the field sampling campaigns and the station characteristics have previously been described in Broman et al. (2020). In brief, three box core casts were performed at each of the four stations located in the Eastern Gotland Basin, Baltic Sea (Fig. 1), and each box core was subsampled with a sediment core ($n = 3$ biological replicates). The top 0–2 cm surface sediment was collected from the sediment cores, homogenized, transferred into liquid nitrogen, and stored at −80°C until DNA and RNA extraction. The stations at which sediments were collected are located along gradients in water depth and oxygen concentration at the sediment–water interface with oxic conditions at Sta. A (60 m depth, 330 μM O_2), hypoxic conditions at Sta. D (130 m, 8.8 μM O_2) and E (170 m, 1.9 μM O_2), and anoxic conditions at Sta. F (210 m, 0 μM O_2). In this study, we define the redox conditions of the 0–2 cm surface sediments (from which DNA and RNA were extracted) based on the vertical sediment microprofiles of dissolved O_2 and H_2S (Broman et al. 2020). The 0–2 cm sediment is therefore considered oxic-anoxic for Sta. A (i.e., having a thin oxygenated surficial layer followed by oxygen-deficient sediment), hypoxic-sulfidic for Sta. D and E, and anoxic-sulfidic for Sta. F (Supplementary Table S1).

Detailed descriptions of the study sites (Fig. 1) have previously been published (Broman et al. 2020) and is here only presented briefly. Oxygen was present at high concentrations

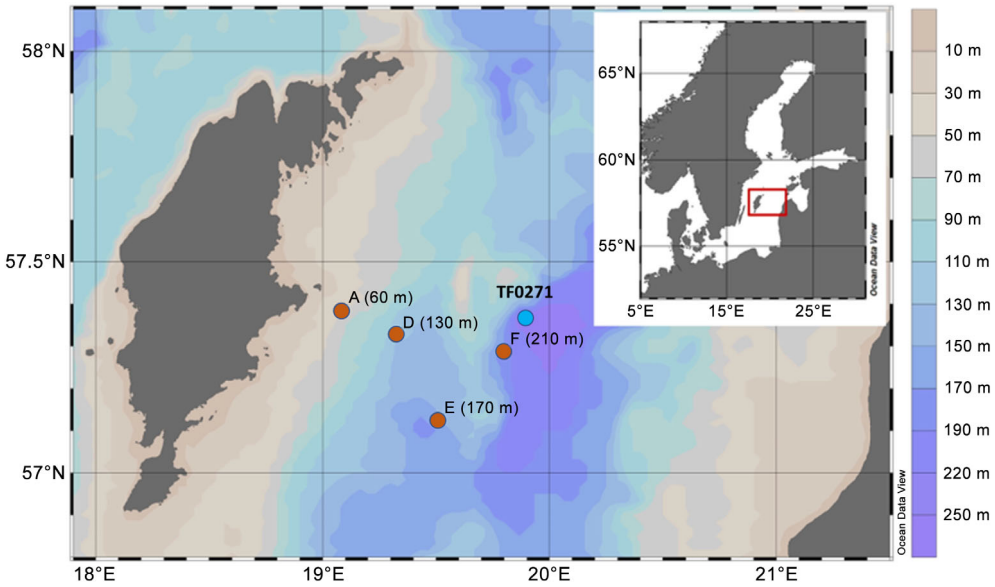

Fig. 1. Location of study sites in the Baltic Sea. A, D, E, and F correspond to the sediment stations (brown dots). TF0271 (blue dot) correspond to the station at which water samples were previously analyzed for the presence of *hgc*-like genes (Capo et al. 2020).

(> 300 μM) at the sediment surface at Sta. A, while hypoxic conditions (8.8 μM) and near-anoxic conditions (1.9 μM) were recorded at Sta. D and E, respectively, and no O_2 (anoxic conditions) was detected at Sta. F (Supplementary Table S1). Anoxic conditions however developed along the 0–2 cm depth profiles also for the three sediment Sta. A, D, and E although at different depths. Dissolved sulfide concentration was close to or below detection limit at Sta. A. In contrast, high sulfide concentrations were found in the three other stations from 0.5 cm sediment depth with the highest concentration at Sta. D (up to 84 μM H_2S at 1.5 cm depth). The concentrations of N_2O were one to two orders of magnitude lower at Sta. A (up to 19 nM) and Sta. F (up to 29 nM) compared to Sta. E (up to 471 nmol L^{-1}) (not measured at Sta. D).

Nucleic acid extraction and sequencing

DNA was extracted from ~ 10 g sediment with the DNeasy PowerMax Soil kit (QIAGEN) and RNA from ~ 2 g sediment with the RNeasy PowerSoil kit (QIAGEN), following the manufacturer's instructions. The TURBO DNA-free kit (Invitrogen) was used to DNase treat extracted RNA and remove DNA contamination. This was followed by bacterial ribosomal RNA depletion using the RiboMinus Transcriptome Isolation Kit (ThermoFisher Scientific). The final quantity and quality of extracted nucleic acids were measured on a NanoDrop One spectrophotometer (ThermoFisher Scientific). Library preparation of DNA and RNA for sequencing was performed with the ThruPLEX DNA-seq (Rubicon Genomics) and TruSeq RNA Library Prep v2 (Illumina) kits, respectively. The samples were sequenced with a paired-end 2 × 150 bp setup at the Science for Life Laboratory Genomics Platform on one Illumina NovaSeq6000 S2 lane (DNA) and one Illumina NovaSeq6000 S4 lane (RNA). That the samples meet the requirements for quantity, quality, and contamination for sequencing was controlled by the SciLifeLab upon sample delivery. Sequencing yielded on average 41 million sequences (DNA samples) and 82 million sequences (RNA samples). A full list of sample names, number of sequences yielded before and after quality trimming, number of contigs assembled, and number of 16S rRNA gene sequences extracted is available in Supplementary Table S3.

Quality trimming

Illumina adapters and PhiX sequences were removed from the raw .fastq sequences using SeqPrep 1.2 (St John 2011) and by mapping reads with bowtie2 2.3.4.3 against the PhiX genome (NCBI Reference Sequence: NC_001422.1; Langmead and Salzberg 2012). Trimmomatic 0.36 was used to quality trim the data with the following parameters: LEADING:20 TRAILING:20 MINLEN:50 (Bolger et al. 2014). The final quality was validated by combining FastQC 0.11.5 (Andrews 2010) reports with MultiQC 1.7 (Ewels et al. 2016). The final DNA quality trimmed data consisted on average of 39.9 million sequences with a length of 137 bp, and the RNA data on average of 81.2 million read-pairs with a length of 144 bp. The final data had an average phred score of 36 per read.

Metagenome assembly and mapping of RNA-seq sequences

The paired-without-unpaired (PwU) output from trimmomatic was used with the assembler MEGAHIT 1.1.2 (Li et al. 2016) using default settings. The metagenome assembly of the DNA samples yielded 12,274,484 contigs with an average length of 665 bp (min: 200 bp, max: 240,752 bp). This was followed by

annotation of the contigs with the Prokka 1.12 software tool (Seemann 2014) that uses Prodigal 2.6.3 (coding sequence translation table 11) for prokaryotic gene prediction (Hyatt et al. 2010) and BLAST 2.6.0+ (Altschul et al. 1990) for sequence alignment of translated nucleotides. Prokka was run with a metagenome setup against the UniProtKB/Swiss-Prot protein database (database downloaded: 31 January 2019) with the following settings: --proteins uniprot_sprot.fasta --metagenome. The DNA and RNA PwU reads were mapped against the contigs with bowtie2, and the resulting .sam files were converted to .bam files using samtools 1.9 (Li et al. 2009). On average, 11,379,819 DNA sequences and 3,550,690 RNA sequences were mapped onto the assembly. The .bam files and the Prokka output .gff file were used to estimate sequence counts by using htseq-count in the HTSeq python package 0.9.1 (Anders et al. 2015) with the following settings: -s no -f bam -t CDS -i ID. The data were normalized as gene length corrected trimmed mean of M-values (GeTMM; Smid et al. 2018) and the results are available in Supplementary Data S1.

Taxonomic annotation

SSU rRNA gene sequences were extracted from the quality trimmed DNA data using SortMeRNA 2.1b with the supplied reference databases (Kopylova et al. 2012). This was followed by taxonomically classification against the small-subunit SILVA database (SSU Ref v132 NR 99) using Kraken2 2.0.7 with default settings (Wood et al. 2019). To estimate relative abundances of taxa, the Kraken2 output reports were analyzed with Bracken 2.5 with the following settings: -r 150 -l G, that is, read length of 150 bp and minimum taxonomic level set to genus (Lu et al. 2017). The default setting of a threshold of 10 counts per genus was used with Bracken 2.5. The final bracken reports were combined into a biom-format file using the python package kraken-biom 1.0.1, with the following setup: ---fmt hdf5 --max D --min G. Finally, the python package biom-format 2.1.7 (McDonald et al. 2012) was used to convert the biom file to a text table. The 16S rRNA gene sequences extracted from the DNA samples yielded on average 15,371 read counts per sample.

Detection of *hgc*-like genes in metagenomes and metatranscriptomes

We first looked for *hgc* gene homologs in the 7,012,761 prodigal predicted genes with the function hmmsearch from hmmer software (3.2.1 version; Finn et al. 2011) and using the HMM profiles from the Hg-MATE database (v1.01142021) built from multiple sequences alignments of *hgcA* and *hgcB* amino acid sequences. We considered genes with E-values $\leq 10^{-3}$ as significant hits resulting in 11,930 hits. To identify which of the 11,930 genes truly correspond to *hgcA* and *hgcB* genes, we used the knowledge from the seminal paper of Parks et al. (2013) that described unique motifs from *hgcA* (NVWCA(A/G/S)GK) and *hgcB* genes (C(M/I)EC(G/S)(A/G)C) and performed a manual check of the presence of *hgcA*-like genes in our dataset resulting in 102 confirmed *hgcA*-like genes being identified. For 71 of them, *hgcB*-like genes were found side-by-side in the same contig. In this work, we called the detected genes *hgc*-like genes because their role in Hg methylation could not be verified solely based on environmental genomics data. Meanwhile, we applied the stringent cutoffs described above to ensure that these genes should be able to perform Hg methylation, based on the current state of knowledge (Parks et al. 2013).

To calculate the proportion and distribution of *hgc*-like genes, only data from *hgcA*-like genes were considered. For normalization, the number of *hgcA*-like genes and transcripts was divided by the total number of prokaryotic DNA sequences and prokaryotic mRNA, respectively. The data were then multiplied by 1 million and reported as counts per million (CPM). Shapiro–Wilk tests were performed to confirm that the data were normally distributed. To identify differences in the total proportion of *hgcA*-like genes and transcripts from each station, we used separate one-way ANOVAs with Tukey's post hoc tests using R aov and TukeyHSD functions from R software. To test if there was a difference in the distribution of *hgcA*-like genes and transcripts (and related microbial groups) between the stations, PERMANOVA tests (9999 permutations) were conducted in the software Past 3.22 (Hammer et al. 2001).

Taxonomic affiliations of *hgc*-like genes

To perform taxonomic identification of *hgcAB*-like gene pairs and *hgcA*-like genes, we used the amino acid sequences of *hgc* genes compiled in Hg-MATE database (v1.01142021; Gionfriddo et al. 2021). For each phylogenetic analysis, the amino acid sequences were aligned using MUSCLE. RAxML (v8.2.10) was used to generate maximum likelihood tree under the GAMMA distribution with the LG model with the following parameters: raxmlHPC -f a -p 283976 -m PROTGAMMAAUTO -N autoMRE -x 2381 -T 10 (Stamatakis 2014). Branch support was generated by rapid bootstrapping. For both phylogenetic trees, RogueNaRok (v1.0) was used to remove "rogue taxa" interfering with proper tree generation (Aberer et al. 2013) Rogue taxa were classified using pplacer and included in the analysis (Matsen et al. 2010). When possible, the taxonomic affiliations of the *hgc*-like genes detected in Baltic Sea sediments were identified at the genus level (Supplementary Table S2). Each *hgc*-like gene detected in Baltic Sea sediments got the label BSS for Baltic Sea Sediments (e.g., BSS_001).

Results

Composition and metabolism of the prokaryotic community

Based on the analysis of 16S rRNA genes extracted from metagenomes in the homogenized 0–2 cm sediment layers, we found that microbial communities from the sampled four stations

mainly consisted of Gammaproteobacteria, Desulfobacterota (Deltaproteobacteria in NCBI classification), Firmicutes, and Bacteroidetes (Supplementary Fig. S1). Both Gammaproteobacteria and Bacteroidetes made up a larger proportion of the total community in the metagenomes from Sta. A (38 ± 1 and 14 ± 1 mean $\pm$ SD in % relative abundance, respectively) compared to Sta. D–F ($15\% \pm 6\%$ and $4\% \pm 1\%$, respectively). In contrast, Firmicutes and Desulfobacterota had a higher relative abundance in metagenomes from Sta. D–F ($27\% \pm 6\%$ and $25\% \pm 4\%$, respectively) as compared to Sta. A ($10\% \pm 1\%$ and $14\% \pm 1\%$, respectively). Chloroflexota (Chloroflexi in NCBI classification) and Spirochaetes also had a higher relative abundance in these three stations (D–F) ($6\% \pm 2\%$ and $3\% \pm 0\%$, respectively) compared to Sta. A ($3\% \pm 0\%$ and $1\% \pm 0\%$, respectively) (Supplementary Fig. S1).

Metagenomes and metatranscriptomes were used to evaluate the presence and expression of functional genes in studied sediment stations. We focused on two of the most important biochemical pathways, the nitrogen and sulfur cycles. Denitrification genes found in the sediment surface (0–2 cm) were affiliated with Alpha-, Beta-, and Gammaproteobacteria (Supplementary Data S1). RNA transcripts affiliated with genes coding for nitrate reduction to nitrite (*narGZHY*, *nxrAB*, and *napAB*) had significantly higher (false discovery rate < 0.05, edgeR analysis; Supplementary Fig. S2A) GeTMM in the sediment from Sta. A compared to the rest. *napA* was significantly higher at Sta. E compared to that in Sta. D and F. RNA transcripts for nitrite reduction to nitric oxide (genes *norBC*) was highest at Sta. E Supplementary Fig. S2B). The reduction processes of (1) nitric oxide to nitrous oxide (*nirKS*) and (2) nitrous oxide to nitrogen (*nosZ*) had the highest GeTMM values at Sta. A, followed by Sta. E (Supplementary Fig. S2C,D). Full pathways for sulfate reduction to sulfide were also available in the RNA transcripts dataset, with dissimilatory sulfate reduction to sulfide being prominent in the sediment of all stations when compared to biological assimilation of sulfate (Supplementary Fig. S2E–G). RNA transcripts affiliated with genes involved in dissimilatory sulfate reduction had significantly higher GeTMM values at A when compared to D and F (genes *aprAB*), as well as A–D, E, and F (genes *dsrAB*) (Supplementary Fig. S2E–G). The UniProtKB annotation results indicated that the microbial taxa conducting dissimilatory sulfate reduction belonged to the archaeal phyla Euryarchaeota and bacterial phyla Alpha-, Delta-, and Gammaproteobacteria (Supplementary Data S1).

Overall proportion of *hgc*-like genes and transcripts

From the 7,012,761 predicted genes detected in the 12 metagenomes obtained from Baltic Sea sediments, we found 102 *hgcA*-like genes including 71 found side-by-side with *hgcB*-like genes on the same contig (Supplementary Table S2). Further analysis is based on proportion values of *hgcA*-like genes only. In the metagenomes, lower *hgcA*-like gene proportion values were observed for Sta. A (mean $\pm$ SD; 83 ± 3 CPM) compared to the Sta. D–F ($171–175 \pm 2–6$ CPM) (Table 1), this difference being significant according to a one-way ANOVA and Tukey post-hoc tests (ANOVA, df = 3, $F = 382$; $p < 0.001$). Although the proportion of detected *hgcA*-like genes was very similar between replicate samples from the same station, we observed a substantial variability between replicate samples in the proportion of the transcripts (Table 1) expressed from 27 of the 102 *hgcA*-like genes (Supplementary Table S2). The combined relative abundances of different *hgcA*-like transcripts ranged from 53 to 103 CPM (SD 10–62 CPM) of total transcripts and was not significantly different between stations (ANOVA, df = 3, $F = 1$; $p = 0.47$).

Taxonomic identification and distribution of *hgc*-like genes and transcripts in Baltic Sea sediments

Two phylogenetic trees were performed: (1) for the 71 *hgcAB*-like gene pairs (Fig. 2; Supplementary Fig. S3) and (2) for the 31 *hgcA*-like genes alone (Supplementary Fig. S4). The *hgc*-carrying microorganisms were affiliated with members of Desulfobacterota, notably within the orders Desulfobacterales and Desulfatiglandales and uncultured members of OalgD group (Table 2). Other *hgc*-carrying genes were identified as likely encoded by members of Bacteroidetes (7 *hgc*-like genes), Chloroflexota (4 genes), and Verrucomicrobia (3 genes). In addition, a majority of *hgc*-like genes were detected in phylogenetic clusters composed of microbial lineages from various phyla. In the present work, we assigned them as cluster U1

Table 1. Proportion of *hgcA*-like genes and transcripts related to the total sequence counts of each metagenome and metatranscriptome obtained from the four stations. For each station, we present the mean, standard deviation, minimum, and maximum values of summed relative abundance of *hgcA*-like genes.

	Metagenomes				Metatranscriptomes			
Relative abundance (in CPM)	Mean	Standard deviation	Min	Max	Mean	Standard deviation	Min	Max
Sta. A	83	3	81	86	87	62	17	138
Sta. D	174	5	170	179	53	10	41	60
Sta. E	175	2	172	176	49	35	17	86
Sta. F	171	6	164	174	103	59	52	168

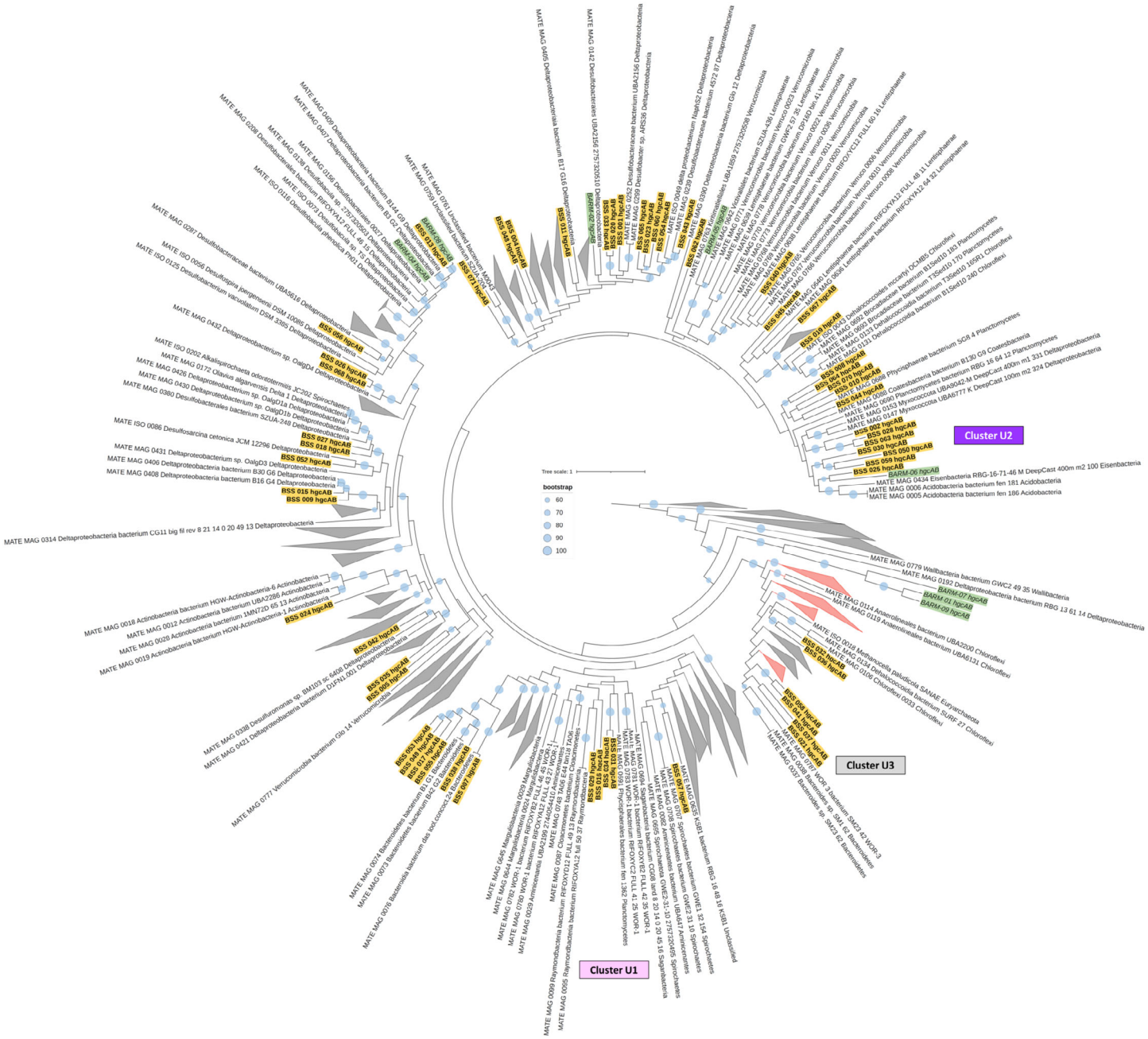

Fig. 2. Simplified phylogenetic tree based on the concatenated amino acid sequences of *hgcAB* genes compiled in the Hg-MATE database (Gionfriddo et al. 2021) and *hgcAB*-like genes detected in Baltic Sea sediments (BSS id). The h*gcAB*-like gene pairs detected in the Baltic Sea water column (BARM id) were also included in this phylogenetic analysis.

(5 genes), cluster U2 (17 genes), and cluster U3 (4 genes) (Fig. 2, Supplementary Figs. S3 and S4).

Among the 20 most abundant *hgc*-like genes detected in the metagenomes (Supplementary Table S2), 13 were affiliated with Desulfobacterota from Desulfobacterales (4 genes), Desulfatiglandales (3 genes from NaphS2), uncultured Desulfobacterota named OlgaD (3 genes), and 3 unidentified. Two other abundant genes were associated with Verrucomicrobia and 1 to Chloroflexota (Dehalococcoidia). The remaining genes were detected in cluster U1 (2 genes) and cluster U2 (2 genes). In the phylogenetic trees, the two abundant *hgc*-like genes found in cluster U2 (genes BSS 070 and BSS 076) were closely related to Planctomycetes (Fig. 2; Supplementary Figs. S3 and S4). The closest relatives of the two most abundant genes detected in

Table 2. Number and proportions (in counts per million, i.e., CPM) of *hgcA*-like genes (metagenomes) and transcripts (metatranscriptomes) for each taxonomic group (with the lowest taxonomic classification shown after the underscore). Based on the phylogenetic analysis, unclassified genes that clustered together in the phylogenetic analysis were categorized into three clusters U.

	Metagenomes		Metatranscriptomes	
Taxonomic groups	**#genes**	**CPM**	**#genes**	**CPM**
Acidobacteria	1	4	0	0
Actinobacteria	1	11	0	0
Bacteroidetes	7	48	0	0
Chloroflexota_Anaerolineales	2	10	0	0
Chloroflexota_Dehalococcoidia	2	11	2	44
Desulfobacterota_Others	13	239	4	70
Desulfobacterota_Desulfarculales	1	6	0	0
Desulfobacterota_Desulfatiglandales	5	75	5	173
Desulfobacterota_Desulfobacterales	11	400	4	181
Desulfobacterota_Desulfobulbales	1	7	0	0
Desulfobacterota_Desulforomonadales	1	15	0	0
Desulfobacterota_Desulfovibrionales	2	14	0	0
Desulfobacterota_Syntrophobacterales	1	9	1	9
Desulfobacterota_UnculturedOalgD	4	233	4	213
Euryarchaeota_Methanocellales	1	9	0	0
Euryarchaeota_Methanomicrobiales	1	6	0	0
Firmicutes	3	16	0	0
Lentisphaerae	3	33	0	0
Nitrospirae	1	6	0	0
Planctomycetes	2	13	0	0
Saganbacteria	2	3	0	0
Spirochaetes	2	20	0	0
Verrucomicrobia	3	341	0	0
Cluster_U1	5	90	3	104
Cluster_U2	17	121	3	76
Cluster_U3	4	34	0	0
Unclassified	6	31	1	7
Total	102	1808	27	878

cluster U1 (BSS_29 and BSS_34) were members of Planctomycetes and Raymondbacteria, respectively. In the metatranscriptomes, 14 of the 20 most abundant *hgc*-like transcripts were identified as Desulfobacterota, with the remaining transcripts affiliated with Chloroflexota (2 genes from Dehalococcoidia) and not taxonomically described microbes (2 genes in cluster U1 and 2 genes in U2) (Supplementary Table S2).

Differences in the distribution of *hgc*-like genes and transcripts between stations

PERMANOVA tests of all 12 samples highlighted significant differences between-stations with regards to the distribution of *hgc*-like genes ($_{pseudo}F = 22.67$, $p < 0.001$) but not transcripts ($_{pseudo}F = 1.32$, $p = 0.082$). In terms of proportions (hereafter mean ± SD, values in CPM) *hgc*-like genes detected in the metagenomes from the Sta. A were mostly attributed to members of uncultured Desulfobacterota OalgD (26 ± 2), and cluster U1 (10 ± 1) (Fig. 3A). In comparison to Sta. A, higher proportions of *hgc*-like genes affiliated with Desulfobacterales (26–39 ± 1–4), Verrucomicrobia (25–49 ± 3–9), and the Cluster U2 (12–15 ± 1–3) were found in metagenomes from Sta. D–F (Fig. 3A).

The distribution of *hgc*-like transcripts also differed among the four stations. For Sta. A, the *hgc*-like transcripts were mainly identified as Desulfobacterales (87 ± 62) and uncultured Desulfobacterota from OalgD group (38 ± 27) and genes closely related to *Desulfobacula* sp. For Sta. D and E, *hgc*-like transcripts associated with members of Desulfobacterota and more specifically Desulfatiglandales (NaphS2, 10–30 ± 17–29) were predominant (Fig. 3B) in accordance with their detected proportion in the metagenomes (Fig. 3A). In the metatranscriptomes from Sta. F, *hgc*-like transcripts from clusters U1 (27 ± 38) and U2 (23 ± 16) were predominant. Finally, *hgc*-like transcripts affiliated to uncultured Desulfobacterota OalgD4 were also

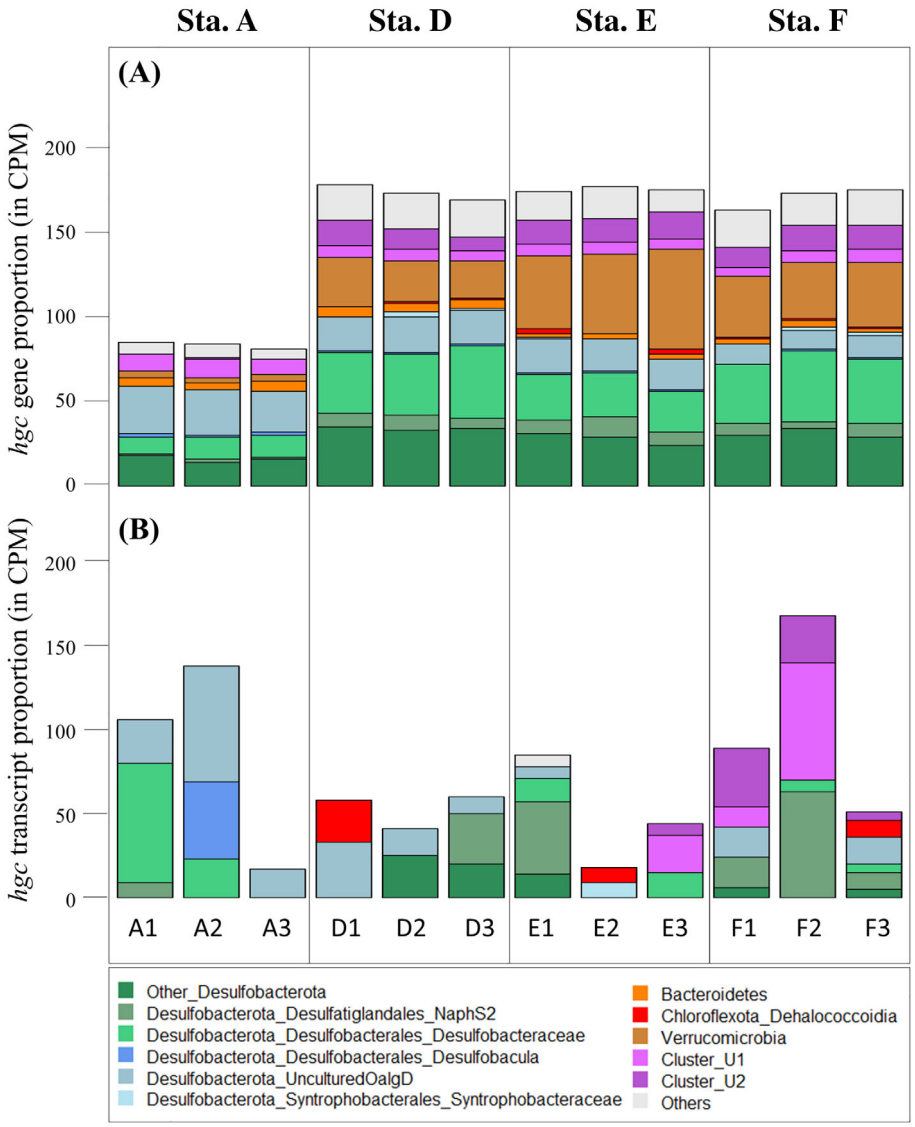

Fig. 3. Proportion of *hgcA*-like genes or transcripts (in CPM) in each taxonomic group in metagenomes (**A**) and metatranscriptomes (**B**) obtained from the four stations. The *hgcA*-like genes labeled as "Others" in the figure correspond to those that account for less than 7.5% of the proportion of *hgc*-like genes in the whole dataset (Supplementary Table S2). For each station, the three replicates are annotated 1, 2, and 3 (e.g., A1, A2, and A3 for Sta. A).

relatively abundant in metatranscriptomes from Sta. D–F (2–20 ± 4–12) (Fig. 3B).

Discussion

Desulfobacterota, Verrucomicrobia, and uncharacterized prokaryotes dominate the diversity of putative Hg methylating microbial groups in Baltic Sea sediments

Most of the *hgc*-like genes detected in the Baltic Sea sediments belong to the orders Desulfobacterales, Desulfatiglandales, and uncultured Desulfobacterota (Table 2). Both Desulfobacterales and Desulfatiglandales are well known to contain sulfate-reducing bacteria. Additionally, *hgc*-like genes associated to Desulfobacterales have previously been detected in coastal Baltic Sea sediments (Värtahamnen port, 21 m water depth; Podar et al. 2015). In this metagenome, Podar et al. (2015) also identified *hgc*-carrying Geobacterales, Firmicutes, and Methanomicrobiales while we unveiled the presence of different *hgc*-carrying groups, that is, Bacteroidetes Verrucomicrobia and Chloroflexota. Differences between the identification of potential Hg methylators by our study and Podar et al. (2015) can be partially explained by differences in the type of sediments collected in the Baltic Sea and by a recent methodological refinement in the phylogenetic diversity and annotation of *hgc*-carrying microbes (Gionfriddo et al. 2019, 2020; McDaniel et al. 2020). Indeed, the recent screening of thousands of metagenomes-assembled genomes for *hgc*-like genes by McDaniel et al. (2020) enabled the detection of hundreds of potential Hg methylators from diverse lineages. In the present

study, certain *hgc*-like genes could not be assigned to specific taxa because their amino acid sequences were embedded in phylogenetic clusters with sequences from various microbial lineages (clusters U1, U2, and U3) (Fig. 2). This illustrates the need of further works to describe better marine microbial communities using, for example, methods such as long read sequencing to get deeper insight into the taxonomy of potential Hg methylators.

Contrasting proportion and distribution of *hgc* gene and transcript depending on sediment redox conditions

The work of Beldowski et al. (2014) showed negative correlations between MeHg concentrations and the redox potential in Baltic Sea sediments and suggested that these relationships were caused by differences in Hg speciation—and thus availability for methylation—related to redox conditions. Our results imply that the relationships between redox conditions and the presence of potential Hg methylators could also explain higher MeHg concentrations in sediments with oxygen deficiency or depletion. For instance, a significantly lower proportion of *hgc*-like genes was found at the sediment with an oxygenated surface (Sta. A) when compared to the sediments with a hypoxic-anoxic surface (Sta. D–F). DNA and RNA, extracted from homogenized 0–2 cm top sediment samples, represent an integrated view of the active microbial community across different redox gradients for the different sediments (Supplementary Table S1). As MeHg formation is known to occur predominantly at oxygen-deficient conditions (Bravo and Cosio 2019), *hgc*-like microbes from Sta. A thus likely originated from oxygen-deficient zones of the 0–2 cm sediments. In contrast to *hgc*-like genes, there were no statistically significant differences in the proportion of *hgc*-like transcripts among stations. In general, the proportion of specific transcripts is expected to be more sensitive to spatial and temporal variations in biogeochemical conditions compared to corresponding genes. Also, as RNA can be rapidly degraded in the environment, the transcripts are more representative of short-term processes (e.g., minutes) while the genes may be more reflective of the performance of a microbial process integrated over longer timescale (from hours to days) (Rocca et al. 2015).

A taxonomic shift in *hgc*-like transcripts from Desulfobacterota members was detected comparing Sta. A, featuring Desulfobacterales and uncultured Desulfobacterota, to Sta. D–F featuring Desulfatiglandales. Interestingly, this shift was accompanied with a compositional shift in sulfate reduction (*drsAB*) transcripts (Supplementary Fig. S2A and Supplementary Data S1). This latter group was, however, not identified as a dominant microorganism carrying *hgc*-like genes in our study (Table 2).

There was a considerably higher *hgc* gene proportion from Verrucomicrobia, clusters U1 and U2 in the hypoxic-anoxic/sulfidic sediments. The *hgc*-carrying members of the PVC superphylum—composed of members of the phyla Planctomycetes, Verrucomicrobia, and Chlamydiae—have been recently reported in various oxygen-deficient environments (Jones et al. 2019; Peterson et al. 2020; Lin et al. 2021). However, they are still poorly described in brackish and marine sediments (exception of Azaroff et al. 2020). Chloroflexota carrying *hgc* genes were recently identified in marine sediments by cloning and sequencing approaches, suggesting that their widespread distribution and potential importance for Hg methylation in marine sediments (Azaroff et al. 2020). A certain proportion of transcripts (*see* Fig. 3) from clusters U1 and U2—not precisely taxonomically identified with the phylogenetic approach—were found to be more predominant in the oxygen-deficient sediments from Sta. D–F compared to the more oxygenated sediment from Sta. A.

The identification of populations carrying and expressing *hgc* genes and their metabolic capacities could provide further insights about how changes in environmental conditions regulate *hgc* gene expression. Additionally, further investigations of the relationship between *hgc* gene expression and MeHg formation (i.e., Hg methylation rates and MeHg concentrations) could provide a refined understanding of the environmental conditions regulating Hg cycling in marine sediments.

Similarity and differences between water and sediment Hg-methylating microbial groups

A previous study (Capo et al. 2020) described *hgc*-like carrying microbes from water samples collected at a station near the sediments included in the present study (TF0271; Fig. 1). Baltic Sea anoxic waters contain predominantly *hgc*-carrying Desulfobacterota, Spirochaetes-like and Kiritimatiellaeota-like bacteria (Capo et al. 2020) and although no identical *hgc*-like genes were found in the two studies, a noteworthy similar taxonomic affiliation of *hgc*-carrying microbes was found between sediment (the present study) and the water (Capo et al. 2020) sample in the Central Baltic Sea. Interestingly, *hgc*-carrying Desulfobacterales, such as *Desulfobacula* sp, were found relatively abundant in both systems. The *hgc*-carrying Spirochaetes-like bacteria and Desulfobulbales known to be predominant in oxygen-depleted waters and settling particles from the Baltic Sea (Capo et al. 2020) were also found to be present in the sediment samples although in low numbers (Table 2). Noticeably, *hgc*-carrying Verrucomicrobia were predominant in both oxygen-deficient water and sediments but were less abundant in sediment with an oxic overlying water zone (i.e., Sta. A) (Fig. 3). Interestingly, no *hgc*-like transcripts from members of this phylum were seen in sediments (Fig. 3), indicating that despite being present they were not active (i.e., they did not express) when the sampling was performed. This finding highlights the importance of investigating both the occurrence of *hgc* genes and their expression for determining the potential role of Hg-methylating microbes in the environment.

Conclusions

The formation of oxygen-deficient regions of the seafloor is accelerating due to anthropogenic eutrophication of

miscellaneous water bodies. Notably, the oxygen-deficient zone in the Baltic Sea has expanded dramatically during the last 30 yr and is one of the largest in the world. Here, we have shown that hypoxic-anoxic/sulfidic conditions select for active Hg-methylating prokaryotes that are different from those that reside in sediments with an oxygenated sediment–water interface. The *hgc*-like transcripts detected in sulfidic sediments had higher *hgc*-like gene proportions of populations with unresolved taxonomy and metabolic features. We describe here for the first time the presence of these uncharacterized prokaryotes, whose current and future impact on MeHg production in marine sediments is so far unknown. Our results highlight the relevance to better describe these expanding and vulnerable systems and determine the physico-chemical variables that control the microbial lineages that are active, their functional traits, and their Hg methylation capacity, in order to better predict the impact of expansion of oxygen-deficient zones on MeHg formation and the associated risks for aquatic ecosystems.

Data Availability Statement

The raw sequence data that support the findings in this study have been deposited online and can be accessed at the NCBI BioProject PRJNA531756.

References

Aberer, A. J., D. Krompass, and A. Stamatakis. 2013. Pruning rogue taxa improves phylogenetic accuracy: An efficient algorithm and webservice. Syst. Biol. **62**: 162–166. doi:10.1093/sysbio/sys078

Altschul, S. F., W. Gish, W. Miller, E. W. Myers, and D. J. Lipman. 1990. Basic local alignment search tool. J. Mol. Biol. **215**: 403–410. doi:10.1016/S0022-2836(05)80360-2

Anders, S., Pyl, P., and Huber, W. 2015. HTSeq—a Python framework to work with high-throughput sequencing data. academic.oup.com

Andrews, S. 2010. FastQC: A quality control tool for high throughput sequence data.

Azaroff, A., M. Goñi Urriza, C. Gassie, M. Monperrus, and R. Guyoneaud. 2020. Marine mercury-methylating microbial communities from coastal to Capbreton Canyon sediments (North Atlantic Ocean). Environ. Pollut. **262**: 114333. doi:10.1016/j.envpol.2020.114333

Azaroff, A., E. Tessier, J. Deborde, R. Guyoneaud, and M. Monperrus. 2019. Mercury and methylmercury concentrations, sources and distribution in submarine canyon sediments (Capbreton, SW France): Implications for the net methylmercury production. Sci. Total Environ. **673**: 511–521.

Beldowski, J., M. Miotk, M. Beldowska, and J. Pempkowiak. 2014. Total, methyl and organic mercury in sediments of the Southern Baltic. Mar. Pollut. Bull. **87**: 388–395. doi:10.1016/j.marpolbul.2014.07.001

Bolger, A., M. Lohse, and B. Usadel. 2014. Trimmomatic: A flexible trimmer for Illumina sequence data. Bioinformatics **30**: 2114–2120. doi:10.1093/bioinformatics/btu170

Bowman, K. L., and others. 2020. Distribution of mercury-cycling genes in the Arctic and equatorial Pacific Oceans and their relationship to mercury speciation. Limnol. Oceanogr. **65**: S310–S320.

Bowman, K. L., C. H. Lamborg, and A. M. Agather. 2020. A global perspective on mercury cycling in the ocean. Sci. Total Environ. **710**: 136166.

Bravo, A., and others. 2018. Methanogens and iron-reducing bacteria: The overlooked members of mercury-methylating microbial communities in Boreal Lakes. Appl. Environ. Microbiol. **84**: 1–16.

Bravo, A. G., and C. Cosio. 2019. Biotic formation of methylmercury: A bio–physico–chemical conundrum. Limnol. Oceanogr. **65**: 1–18.

Bravo, A. G., J. L. Loizeau, P. Dranguet, S. Makri, E. Björn, V. G. Ungureanu, V. I. Slaveykova, and C. Cosio. 2016. Persistent Hg contamination and occurrence of Hg-methylating transcript (hgcA) downstream of a chlor-alkali plant in the Olt River (Romania). Environ. Sci. Pollut. Res. **23**: 10529–10541. doi:10.1007/s11356-015-5906-4

Breitburg, D., and others. 2018. Declining oxygen in the global ocean and coastal waters. Science (80-) **359**: 1–11.

Broman, E., S. Bonaglia, O. Holovachov, U. Marzocchi, P. O. J. Hall, and F. J. A. Nascimento. 2020. Uncovering diversity and metabolic spectrum of animals in dead zone sediments. Commun. Biol. **3**: 106.

Capo, E., and others. 2020. Deltaproteobacteria and spirochaetes-like bacteria are abundant putative mercury methylators in oxygen-deficient water and marine particles in the Baltic Sea. Front. Microbiol. **11**: 1–11.

Christensen, G. A., and others. 2019. Determining the reliability of measuring mercury cycling gene abundance with correlations with mercury and methylmercury concentrations. Environ. Sci. Technol. **53**: 8649–8663. doi:10.1021/acs.est.8b06389

Compeau, G. C., and R. Bartha. 1985. Sulfate-reducing bacteria: Principal methylators of mercury in anoxic estuarine sediment. Appl. Environ. Microbiol. **50**: 498–502. doi:10.1128/aem.50.2.498-502.1985

Conley, D. J., and others. 2012. Hypoxia is increasing in the coastal zone of the Baltic Sea. Environ. Sci. Technol. **45**: 6777–6783.

Diaz, R. J., and R. Rosenberg. 2008. Spreading dead zones and consequences for marine ecosystems. Science (80-) **321**: 926–929. doi:10.1126/science.1156401

Ewels, P., M. Magnusson, S. Lundin, and M. Käller. 2016. MultiQC: Summarize analysis results for multiple tools and samples in a single report. Bioinformatics **32**: 3047–3048. doi:10.1093/bioinformatics/btw354

Finn, R. D., J. Clements, and S. R. Eddy. 2011. HMMER web server: Interactive sequence similarity searching. Nucleic Acids Res. **39**: W29–W37. doi:10.1093/nar/gkr367

Fleming, E. J., E. E. Mack, P. G. Green, and D. C. Nelson. 2006. Mercury methylation from unexpected sources: Molybdate-inhibited freshwater sediments and an iron-reducing bacterium. Appl. Environ. Microbiol. **72**: 457–464. doi:10.1128/AEM.72.1.457-464.2006

Gascón Díez, E., J. L. Loizeau, C. Cosio, S. Bouchet, T. Adatte, D. Amouroux, and A. G. Bravo. 2016. Role of settling particles on mercury methylation in the oxic water column of freshwater systems. Environ. Sci. Technol. **50**: 11672–11679. doi:10.1021/acs.est.6b03260

Gilmour, C. C., G. S. Riedel, M. C. Ederington, J. T. Bell, G. A. Gill, and M. C. Stordal. 1998. Methylmercury concentrations and production rates across a trophic gradient in the northern Everglades. Biogeochemistry **40**: 327–345. doi:10.1023/A:1005972708616

Gionfriddo, C. and others. 2021. Hg-cycling microorganisms in aquatic and terrestrial ecosystems database v1.01142021. doi:10.25573/serc13105370.v1

Gionfriddo, C., M. Podar, C. Gilmour, E. Pierce, and D. Elias. 2019. ORNL compiled mercury methylator database. ORNLCIFSFA (Critical Interfaces Science Focus Area). Oak Ridge National Lab (ORNL). doi:10.1016/j.tplants.2019.08.004

Gionfriddo, C. M., and others. 2016. Microbial mercury methylation in Antarctic sea ice. Nat. Microbiol. **1**: 1–12.

Gionfriddo, C. M., and others. 2020. An improved hgcAB primer set and direct high-throughput sequencing expand Hg-methylator diversity in nature. Front. Microbiol. **11**: 2275.

Goñi-Urriza, M., Y. Corsellis, L. Lanceleur, E. Tessier, J. Gury, M. Monperrus, and R. Guyoneaud. 2015. Relationships between bacterial energetic metabolism, mercury methylation potential, and hgcA/hgcB gene expression in desulfovibrio dechloroacetivorans BerOc1. Environ. Sci. Pollut. Res. **22**: 13764–13771. doi:10.1007/s11356-015-4273-5

Hamelin, S., M. Amyot, T. Barkay, Y. Wang, and D. Planas. 2011. Methanogens: Principal methylators of mercury in lake periphyton. Environ. Sci. Technol. **45**: 7693–7700. doi:10.1021/es2010072

Hammer, Ø., D. A. T. Harper, and P. D. Ryan. 2001. PAST: Paleontological statistics software package for education and data analysis. Palaeontol. Electron. **4**: 9.

Hansson, M., L. Viktorsson, and L. Andersson. 2020. Oxygen survey in the Baltic Sea 2019 - extent of anoxia and hypoxia, 1960-2019. Swedish Meteorological and Hydrological Institute. doi:10.3897/BDJ.8.e59177

Hollweg, T. A., C. C. Gilmour, and R. P. Mason. 2009. Methylmercury production in sediments of Chesapeake Bay and the mid-Atlantic continental margin. Mar. Chem. **114**: 86–101. doi:10.1016/j.marchem.2009.04.004

Hollweg, T. A., C. C. Gilmour, and R. P. Mason. 2010. Mercury and methylmercury cycling in sediments of the mid-Atlantic continental shelf and slope. Limnol. Oceanogr. **55**: 2703–2722. doi:10.4319/lo.2010.55.6.2703

Hu, H., and others. 2020. Shifts in mercury methylation across a peatland chronosequence: From sulfate reduction to methanogenesis and syntrophy. J. Hazard. Mater. **387**: 121967. doi:10.1016/j.jhazmat.2019.121967

Hyatt, D., G.-L. Chen, P. F. LoCascio, M. L. Land, F. W. Larimer, and L. J. Hauser. 2010. Prodigal: Prokaryotic gene recognition and translation initiation site identification. BMC Bioinformatics **11**: 119.

Jones, D. S., G. M. Walker, N. W. Johnson, C. P. J. Mitchell, J. K. Coleman Wasik, and J. V. Bailey. 2019. Molecular evidence for novel mercury methylating microorganisms in sulfate-impacted lakes. ISME J. **13**: 1659–1675. doi:10.1038/s41396-019-0376-1

King, J. K., J. E. Kostka, M. E. Frischer, and F. M. Saunders. 2000. Sulfate-reducing bacteria methylate mercury at variable rates in pure culture and in marine sediments. Appl. Environ. Microbiol. **66**: 2430–2437. doi:10.1128/AEM.66.6.2430-2437.2000

King, J. K., J. E. Kostka, M. E. Frischer, F. M. Saunders, and R. A. Jahnke. 2001. A quantitative relationship that demonstrates mercury methylation rates in marine sediments are based on the community composition and activity of sulfate-reducing bacteria. Environ. Sci. Technol. **35**: 2491–2496. doi:10.1021/es001813q

King, J. K., F. M. Saunders, R. F. Lee, and R. A. Jahnke. 1999. Coupling mercury methylation rates to sulfate reduction rates in marine sediments. Environ. Toxicol. Chem. **18**: 1362–1369. doi:10.1002/etc.5620180704

Kopylova, E., L. Noé, and H. Touzet. 2012. SortMeRNA: Fast and accurate filtering of ribosomal RNAs in metatranscriptomic data. Bioinformatics **28**: 3211–3217. doi:10.1093/bioinformatics/bts611

Kwasigroch, U. 2021. Distribution and bioavailability of mercury in the surface sediments of the Baltic Sea. Environ. Sci. Pollut. Res. **28**: 35690–35708. doi:10.1007/s11356-021-13023-4

Langmead, B., and S. L. Salzberg. 2012. Fast gapped-read alignment with Bowtie 2. Nat. Methods **9**: 357–359. doi:10.1038/nmeth.1923

Li, H., and others. 2009. The sequence alignment/map format and SAMtools. Bioinformatics **25**: 2078–2079. doi:10.1093/bioinformatics/btp352

Li, D., and others. 2016. MEGAHIT v1.0: A fast and scalable metagenome assembler driven by advanced methodologies and community practices. Methods **102**: 3–11. doi:10.1016/j.ymeth.2016.02.020

Lin, H., and others. 2021. Mercury methylation by metabolically versatile and cosmopolitan marine bacteria. ISME J.: **15**: 1810–1825.

Lu, J., F. Breitwieser, P. Thielen, and S. Salzberg. 2017. Bracken: Estimating species abundance in metagenomics data. PeerJ Comput. Sci. **3**: e104. doi:10.7717/peerj-cs.104

Matsen, F. A., R. B. Kodner, and E. V. Armbrust. 2010. pplacer: Linear time maximum-likelihood and Bayesian

phylogenetic placement of sequences onto a fixed reference tree. BMC Bioinformatics **11**: 538.

Mason, R., A. L. Choi, W. F. Fitzgerald, C. R. Hammerschmidt, C. H. Lamborg, and A. L. Soerensen. 2012. Mercury biogeochemical cycling in the ocean and policy implications. Environ. Res. **119**: 101–117. doi:10.1016/j.envres.2012.03.013

McDaniel, E., B. Peterson, S. Stevens, P. Tran, K. Anantharaman, and K. McMahon. 2020. Expanded phylogenetic diversity and metabolic flexibility of mercury-methylating microorganisms. mSystems **5**: 1–21.

McDonald, D., and others. The Biological Observation Matrix (BIOM) format or: How I learned to stop worrying and love the ome-ome. . Gigascience 2012 **1** 7.

Merritt, K. A., and A. Amirbahman. 2009. Mercury methylation dynamics in estuarine and coastal marine environments—a critical review. Earth-Sci. Rev. **96**: 54–66. doi:10.1016/j.earscirev.2009.06.002

Parks, J. M., and others. 2013. The genetic basis for bacterial mercury methylation. Science (80-) **339**: 1332–1335. doi:10.1126/science.1230667

Peñuelas, J., and others. 2019. The bioelements, the elementome, and the biogeochemical niche. Ecology **100**: 1–15.

Peterson, B. D., and others. 2020. Mercury methylation genes identified across diverse anaerobic microbial guilds in a eutrophic sulfate-enriched lake. Environ. Sci. Technol. **54**: 15840–15851. doi:10.1021/acs.est.0c05435

Podar, M., and others. 2015. Global prevalence and distribution of genes and microorganisms involved in mercury methylation. Sci. Adv. **1**: 1–13.

Rocca, J. D., and others. 2015. Relationships between protein-encoding gene abundance and corresponding process are commonly assumed yet rarely observed. ISME J. **9**: 1693–1699. doi:10.1038/ismej.2014.252

Schaefer, J. K., R. M. Kronberg, E. Björn, and U. Skyllberg. 2020. Anaerobic guilds responsible for mercury methylation in boreal wetlands of varied trophic status serving as either a methylmercury source or sink. Environ. Microbiol. **22**: 3685–3699. doi:10.1111/1462-2920.15134

Seemann, T. 2014. Prokka: Rapid prokaryotic genome annotation. Bioinformatics **30**: 2068–2069. doi:10.1093/bioinformatics/btu153

Siedlewicz, G., E. Korejwo, M. Szubska, M. Grabowski, U. Kwasigroch, and J. Bełdowski. 2020. Presence of mercury and methylmercury in Baltic Sea sediments, collected in ammunition dumpsites. Mar. Environ. Res. **162**: 105158. doi:10.1016/j.marenvres.2020.105158

Smid, M., and others. 2018. Gene length corrected trimmed mean of M-values (GeTMM) processing of RNA-seq data performs similarly in intersample analyses while improving intrasample comparisons. BMC Bioinformatics **19**: 236.

Soerensen, A. L., A. T. Schartup, A. Skrobonja, S. Bouchet, D. Amouroux, V. Liem-Nguyen, and E. Björn. 2018. Deciphering the role of water column redoxclines on methylmercury cycling using speciation modeling and observations from the Baltic Sea. Global Biogeochem. Cycles **32**: 1498–1513. doi:10.1029/2018GB005942

Stamatakis, A. 2014. RAxML version 8: A tool for phylogenetic analysis and post-analysis of large phylogenies. Bioinformatics **30**: 1312–1313. doi:10.1093/bioinformatics/btu033

Tada, Y., K. Marumoto, and A. Takeuchi. 2020. Nitrospina-like bacteria are potential mercury methylators in the mesopelagic zone in the East China Sea. Front. Microbiol. **11**: 11.

Tang, W. L., Y. R. Liu, W. Y. Guan, H. Zhong, X. M. Qu, and T. Zhang. 2020. Understanding mercury methylation in the changing environment: Recent advances in assessing microbial methylators and mercury bioavailability. Sci. Total Environ. **714**: 136827.

Villar, E., L. Cabrol, and L. E. Heimbürger-Boavida. 2020. Widespread microbial mercury methylation genes in the global ocean. Environ. Microbiol. Rep. **12**: 277–287. doi:10.1111/1758-2229.12829

Wood, D. E., J. Lu, and B. Langmead. 2019. Improved metagenomic analysis with Kraken 2. Genome Biol. **20**: 257.

Yu, R. Q., J. R. Reinfelder, M. E. Hines, and T. Barkay. 2018. Syntrophic pathways for microbial mercury methylation. ISME J. **12**: 1826–1835. doi:10.1038/s41396-018-0106-0

Acknowledgments

This work was funded by the Swedish Research Council Formas (grants 2018-01031 and 2016-00804); the Swedish Research Council (grants 2015-03717 and 2017-04422); the Swedish Environmental Protection Agency (grant NV-802-0151-18). A.G.B. acknowledges the Marie Curie Individual Fellowship (H2020-MSCA-IF-2016; project-749645). The authors acknowledge support from the National Genomics Infrastructure in Stockholm funded by Science for Life Laboratory, the Knut and Alice Wallenberg Foundation and the Swedish Research Council; SNIC/Uppsala Multidisciplinary Center for Advanced Computational Science for assistance with massively parallel sequencing and access to the UPPMAX computational infrastructure. The bioinformatic analyses were enabled by resources in project SNIC 2018-8-246 provided by the Swedish National Infrastructure for Computing (SNIC) at UPPMAX, partially funded by the Swedish Research Council through grant agreement no. 2018-05973. We thank the captain and crew of the University of Gothenburg R/V Skagerak for skillful help at sea. We are very thankful to Benjamin Peterson (University of Winsconsin-Madison, Madison, WI, USA) for help with phylogenetic analysis.

Conflict of Interest

None declared.

Submitted 25 August 2021
Revised 19 October 2021
Accepted 31 October 2021

Associate editor: Werner Eckert